JGR Atmospheres

RESEARCH ARTICLE
10.1029/2024JD042161

Hemispheric Asymmetry in Stratospheric Trends of HCl and Ozone: Impact of Chemical Feedback on Ozone Recovery

Andreas Chrysanthou[1,2], Kimberlee Dubé[3], Susann Tegtmeier[3], and Martyn P. Chipperfield[1,4]

[1]School of Earth and Environment, University of Leeds, Leeds, UK, [2]Now at: Laboratory of Atmospheric Physics, Aristotle University of Thessaloniki, Thessaloniki, Greece, [3]Institute of Space and Atmospheric Studies, University of Saskatchewan, Saskatoon, SK, Canada, [4]National Centre for Earth Observation, University of Leeds, Leeds, UK

Key Points:

- Atmospheric chemistry experiment - fourier transform spectrometer (ACE-FTS) satellite data and model show asymmetry in stratospheric trends of long-lived tracers, HCl and O_3
- Model-derived sensitivity of O_3 to halogens quantifies the chemical feed-back of dynamics in modifying the lower stratospheric O_3 trends
- Asymmetry in chlorine trends accentuates the midlatitude ozone recovery signal for the southern hemisphere (SH) and delays it in the north

Supporting Information:

Supporting Information may be found in the online version of this article.

Correspondence to:

A. Chrysanthou and M. P. Chipperfield,
a.chrysanthou1@leeds.ac.uk;
m.chipperfield@leeds.ac.uk

Citation:

Chrysanthou, A., Dubé, K., Tegtmeier, S., & Chipperfield, M. P. (2025). Hemispheric asymmetry in stratospheric trends of HCl and ozone: Impact of chemical feedback on ozone recovery. *Journal of Geophysical Research: Atmospheres*, *130*, e2024JD042161. https://doi.org/10.1029/2024JD042161

Received 6 AUG 2024
Accepted 16 JAN 2025

Author Contributions:

Conceptualization: Andreas Chrysanthou, Susann Tegtmeier, Martyn P. Chipperfield
Data curation: Andreas Chrysanthou, Kimberlee Dubé
Formal analysis: Andreas Chrysanthou
Investigation: Susann Tegtmeier, Martyn P. Chipperfield
Methodology: Andreas Chrysanthou, Susann Tegtmeier, Martyn P. Chipperfield
Software: Kimberlee Dubé
Validation: Andreas Chrysanthou, Kimberlee Dubé

Abstract We use trace gas profiles from Atmospheric Chemistry Experiment - Fourier Transform Spectrometer (ACE-FTS) satellite measurements and the TOMCAT three-dimensional chemical transport model to diagnose stratospheric trends in O_3, HCl and N_2O. We find that the 2004–2021 ACE-FTS trends exhibit a clear lower stratosphere (LS) interhemispheric asymmetry with positive (negative) O_3 and N_2O (HCl) trends in the Southern Hemisphere (SH), and trends of opposite sign in the Northern Hemisphere (NH). The trends are larger for the shorter time period of 2004–2018. TOMCAT qualitatively agrees with the ACE-FTS LS N_2O and HCl trends, confirming that transport variability drives such patterns, despite some discrepancies for O_3. An additional model simulation is used to quantify the sensitivity of O_3 to long-term changes in chlorine and bromine and thus determine the chemical contribution of the spatially varying halogen trends to both observed and modeled O_3 trends. Overall, the recent dynamically induced variation in mid-latitude LS halogen abundance has, through chemical feedback, accentuated the O_3 recovery signal in the SH and delayed it in the NH, reflecting the enhanced dynamical variability of the NH. These results further indicate the complexities that exist in the search for the signal of ozone recovery in the mid-latitude LS.

Plain Language Summary It is well known that over the past 50 years, stratospheric ozone has been depleted through increases in the stratospheric loading of chlorine and bromine. Through the action of the Montreal Protocol, the overall total abundance of these halogen species is decreasing. Accordingly, we expect the ozone layer to show signs of recovery from this past depletion. However, in the LS, where O_3 has a photochemical lifetime of many years, it is also affected by dynamical variability. This can introduce multi-year variations into long-term trends. This dynamical variability can also affect the abundance of halogen species, which can drive variations in the chemical loss of ozone. Hence, there is chemical feedback between the dynamically induced variability of ozone and halogens. Here, we demonstrate this dynamical variability in O_3 and HCl using data from the ACE-FTS satellite instrument and quantify the magnitude of this feedback using simulations of a detailed 3-D chemical transport model. We show that dynamical variability of halogen loading has enhanced the signal of lower stratospheric ozone recovery in SH midlatitudes but has delayed it in NH midlatitudes.

1. Introduction

The Montreal Protocol has successfully resulted in reduced emissions of ozone (O_3)-depleting substances (ODSs) thus leading the stratospheric O_3 layer to exhibit some signs of gradual recovery since the turn of the 21st century, notably in the upper stratosphere (US; e.g., Newchurch et al., 2003; Kyrölä et al., 2013; Harris et al., 2015; Chipperfield et al., 2017; Sofieva et al., 2017; Steinbrecht et al., 2017) and the Antarctic (Solomon et al., 2016). In contrast, in the extrapolar lower stratosphere (LS) O_3 is still showing signs of decline (e.g., Ball et al., 2018, 2019), but with different patterns between the two hemispheres depending on the period considered (with some changes not statistically significant).

Despite the decreasing concentrations of chlorine-containing ODSs, HCl, the largest inorganic chlorine (Cly) reservoir, is not declining monotonically and, in the LS, is subject to dynamical variability on a multiyear timescale (Mahieu et al., 2014). Moreover, the trends of HCl (or total inorganic chlorine, Cly) are characterized by a clear hemispheric asymmetry (Mahieu et al., 2014; Strahan et al., 2020) a trait shared, in fact, by most long-lived source gases emitted at the surface and reach the stratosphere such as nitrous oxide (N_2O; Dubé et al., 2023; Strahan et al., 2020), NO_x (Dubé et al., 2020; Galytska et al., 2019) and F_y (Prignon et al., 2021). As it is

10.1029/2024JD042161

Visualization: Andreas Chrysanthou
Writing – original draft: Andreas Chrysanthou, Martyn P. Chipperfield
Writing – review & editing: Andreas Chrysanthou, Kimberlee Dubé, Susann Tegtmeier, Martyn P. Chipperfield

insufficient to attribute this phenomenon to changes in source gas emissions alone, these features have been shown to be mainly determined by characteristics of the Brewer-Dobson circulation (BDC) and its associated transport changes (e.g., Han et al., 2019; Mahieu et al., 2014; Ploeger & Garny, 2022; Stiller et al., 2017) as shifts of the circulation patterns can redistribute HCl (or Cly) and N_2O between the tropical entrainment regions and the subtropics of both hemispheres. In addition to the dynamically induced O_3 variations (e.g., Bognar et al., 2022), chemical feedbacks of, for example, chlorine could modify the O_3 trends.

Under human-induced climate change, increasing greenhouse gases including carbon dioxide (CO_2) and methane (CH_4), are simulated to accelerate the BDC. This change is projected to be countered by an emerging slowdown of the southern hemispheric (SH) circulation in the 21st century due the decreasing ODSs (Abalos et al., 2019; Polvani et al., 2018). Coupled with the large dynamical variability of the LS, this underscores the importance of disentangling the compounding and complex interactions between dynamics, O_3, and other chemically active tracers in order to understand the progress of ozone recovery.

Here we examine observations from the Atmospheric Chemistry Experiment - Fourier Transform Spectrometer (ACE-FTS; Bernath et al., 2005) and modeled trends in stratospheric tracers since 2004, the start of ACE-FTS measurements. In particular, we investigate the contribution of interhemispheric multiannual dynamical variability in the expected halogen (chlorine and bromine) decrease to ozone trends. Section 2 describes the models and datasets used in this study. Section 3 presents our results followed by conclusions in Section 4.

2. Observations and Model

2.1. ACE-FTS Data

Atmospheric chemistry experiment - fourier transform spectrometer is an infrared Fourier transform spectrometer that has been operating from a high inclination orbit on the SCISAT satellite since February 2004 (Bernath et al., 2005; Boone et al., 2005). Atmospheric chemistry experiment - fourier transform spectrometer measures transmitted radiation from 750 to 4,400 cm^{-1} using a solar occultation viewing geometry and observes approximately 30 profiles per day, 15 at sunrise and 15 at sunset. Vertical profiles of over 40 molecules are retrieved from the ACE-FTS transmission observations.

We use N_2O, HCl, and O_3 profiles from version 4.2 of the ACE-FTS retrieval, described in Boone et al. (2020). All observations are filtered according to the data quality flags created by Sheese et al. (2015) before any further analysis is performed. The ACE-FTS profiles are retrieved on an altitude grid; we convert this to a pressure grid using the temperature and pressure profiles that are provided with each ACE-FTS trace gas profile. The area-weighted monthly zonal mean profiles in 10° latitude bands are computed for each of N_2O, HCl and O_3. The monthly zonal mean profiles are then deseasonalized by subtracting the multi-annual mean for a given month of the year from all values for that month within each latitude band and pressure level. Months with fewer than 10 measurements in each latitude/pressure bin are excluded.

2.2. TOMCAT 3-D CTM

We use results from the TOMCAT/SLIMCAT (hereafter TOMCAT) off-line 3-D chemical transport model (CTM; Chipperfield, 2006). The model contains a detailed description of stratospheric chemistry, including heterogeneous reactions on sulfate aerosols and PSCs. Here the model was forced using European center for medium-range weather forecasts ERA5 winds and temperatures (Hersbach et al., 2020) and run with a resolution of 2.8° × 2.8° with 32 levels from the surface to ∼60 km, as in Dhomse et al. (2019). The surface mixing ratios of long-lived source gases (e.g., CFCs, HCFCs, CH_4, N_2O) were taken from WMO (2018) scenario A1 and upper tropospheric chlorinated very short-lived substances (VSLS; e.g. CCl4, CH_3CCl_3, CH_2Cl_2 and C_2Cl_4) are prescribed following Hossaini et al. (2019).

We performed two multidecadal model simulations. The control run (CTL) was spun up from 1977 and integrated until December 2021 including all the standard model dynamical and chemical processes. Sensitivity run PeakH was initialized from CTL in 1995 and integrated until 2021 using constant surface mixing ratios of halogenated ODSs at 1995 peak levels. Comparison of PeakH and CTL is used to calculate the chemical impact on O_3 of the decreasing halogens in run CTL. For the sake of the comparison against observations, we interpolate the TOMCAT output to the same 10° latitude grid that the ACE-FTS data is provided with.

2.3. MLR Model

We employ the latest release (v.0.8.2) of the Long-term Ozone Trends and Uncertainties in the Stratosphere (LOTUS) multiple-linear regression (MLR) model to analyze the post-2004 trends of relevant stratospheric species. As usual in MLR implementation in trend detection, we use known drivers of the O_3, HCl and N_2O variability as explanatory variables in the LOTUS MLR. These include an 11 year solar cycle (10.7 cm solar flux), an El Niño–Southern Oscillation (ENSO; Multivariate ENSO v2 index without lag), two orthogonal components of the quasi-biennial oscillation (QBO1 and QBO2) computed via principal component analysis of the daily Singapore winds, as well as a latitude-resolved stratospheric aerosol optical depth predictor taken from the Global Satellite-based Stratospheric Aerosol Climatology (GloSSAC; Kovilakam et al., 2020). The focus of the study is the post-2004 period hence we only compute a single linear trend for the whole time interval considered. Finally, we deseasonalize the monthly mean ACE-FTS and TOMCAT model output prior to running the MLR for each altitude/latitude bin and we utilize the LOTUS built-in Fourier components to add two seasonal (annual and semi-annual) components for the constant term in the MLR as well as in the two QBO predictors.

3. Results

Figure 1 shows the trend in ACE-FTS O_3, HCl and N_2O, serving as a proxy for trends in stratospheric circulation, for the two periods 2004–2018 and 2004–2021. In the mid-upper quasi-global stratosphere (above 10 hPa), HCl shows a clear negative trend over both periods, with an average value of -4% dec^{-1} over the period 2004–2018 (slightly more negative than the extended 2004–2021 period) reflecting the overall decreasing abundance of stratospheric chlorine due to the Montreal Protocol. The negative chlorine trend feeds onto the increasing O_3 trend reaching an average value of 1.4% dec^{-1} throughout the layer over 2004–2018, however this increasing O_3 trend is more pronounced and statistically significant over the extended period from 2004 to 2021 showing an increase of 0.5% dec^{-1} compared to the 2004–2018 period. This, along with temperature decreases (Steiner et al., 2020), causes a positive trend in O_3, which is larger and more significant for the longer time period. The impacts of chlorine and temperature on O_3 in the US reflect its short chemical lifetime of a few days in this region (Stolarski et al., 2012). The greenhouse gas N_2O has an increasing trend in the troposphere of around 0.3% yr^{-1} from 1980 to 2020 (Prather et al., 2023; Tian et al., 2024). This drives an increase in the mid-US, where the abundance of N_2O becomes small, of over 10% dec^{-1}.

In contrast to the mid-upper stratosphere, the trends in O_3, HCl and N_2O below 10 hPa show distinct inter-hemispheric asymmetries. This signal is very clear in the dynamical tracer N_2O where, over the two time periods analyzed, it shows the expected positive trend in the SH but a decreasing trend in the northern hemisphere (NH). These trends are slightly larger over the shorter period through 2018 and are due to multiannual variability in the transport of the NH cell (Ploeger & Garny, 2022). The trends in HCl, the major component of inorganic chlorine (Cly) which acts as a long-lived tracer, show a similar pattern to N_2O, but with reversed sign as HCl is the product of source gas degradation. Over 2004–2018, the SH cell exhibits a strong negative trend (-4.5% dec^{-1}) and the NH cell a strong positive trend of 3.1% dec^{-1}, however, the interhemispheric asymmetry signal is suppressed over 2004–2021 period, modulated mainly by the decreased positive trend in the NH cell and the reversal of the trend signal in the tropics. In the LS, O_3 is long-lived and displays an interhemispheric asymmetry of trends. O_3 is increasing slightly (i.e., showing signs of recovery) in the SH, but still appears to decrease in the NH (statistically not significant changes), and becomes more positive over the extended 2004–2021 period. Part of this trend asymmetry will be due to the same dynamical variability that is forcing the trends in, for example, N_2O but there is also the potential for feedback of the changing chemical composition on the O_3 abundance, especially the impact of changing halogens. These patterns suggest an overall situation of ozone recovery in the LS quasi-global region, a signal that becomes diluted in the observed O_3 trends through 2021.

The equivalent model trends in O_3 and HCl for the TOMCAT CTL and PeakH simulations for the period 2004–2018 are shown in Figure 2 (Figure S1 in Supporting Information S1 for 2004–2021). The corresponding trends for TOMCAT CTL N_2O, and Age-of-Air (age of air (AoA)) are shown in Figure 3 (Figure S2 in Supporting Information S1 for 2004–2021). The model produces a uniform decrease in HCl in the US, reflecting the decrease in model chlorine loading, corroborating the observed findings. Despite exhibiting a low bias in the US O_3 trend compared to the observed trends (roughly two thirds over 2004–2018 and relatively unchanged with respect to 2004–2021 period) as well as a more negative HCl trend by up to 0.85% dec^{-1} (over both periods considered here) compared to observations in the same region, the model captures the observed hemispheric asymmetry at lower

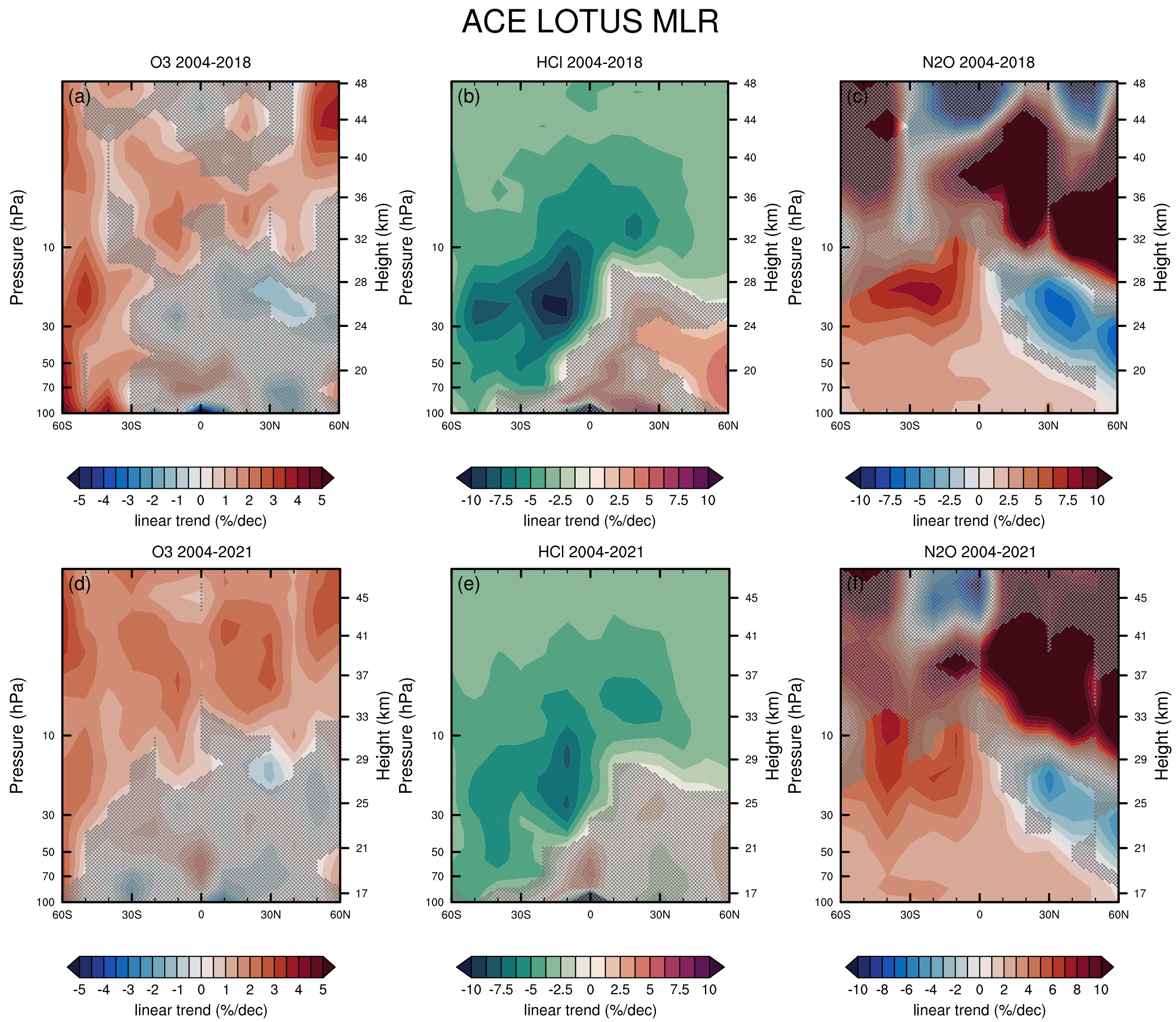

Figure 1. Atmospheric chemistry experiment - fourier transform spectrometer (ACE-FTS) LOTUS multiple-linear regression trends (% dec^{-1}) for (a), (d) O_3 (b), (e) HCl and (c), (f) N_2O over time periods 2004–2018 (top row) and 2004–2021 (bottom row) respectively. Gray stippling indicates where the linear trends are not statistically significant at the 95th percentile.

altitudes with a few notable differences. As seen in the modeled N_2O trends (Figure 3 and Figure S2 in Supporting Information S1), the amplitude of the interhemispheric asymmetry is smaller compared to the observations (Figure 1) throughout both periods, while for both observations and model, this asymmetry is rather muted through 2021. The suppression of the interhemispheric asymmetry through 2021 is clearly reflected for the TOMCAT CTL simulation in the respective AoA trends (Figure 3 and Figure S2 in Supporting Information S1); the older AoA trends arising from the SH mid-latitudes and tropics point to a slow-down of the stratospheric circulation associated with the dynamical variability over the 2019–2021 period.

In the LS, modeled HCl declines at a rate of around −7.5% dec^{-1} in the SH mid-latitudes, which is almost 3% dec^{-1} lower than observations through 2018. In the opposite hemisphere mid-latitudes, modeled HCl positive trend is low biased by approximately the same amount (3% dec^{-1}) compared to the observations, but over 2004–2021, the NH mid-latitudes have smaller model-observation differences, with trends of opposite sign. Moreover, this picture persists in the tropical LS where model and observations exhibit trends of opposite sign with the model showing an overall negative HCl trend (−1.7% dec^{-1} for the model vs. 0.35% dec^{-1} for the observations

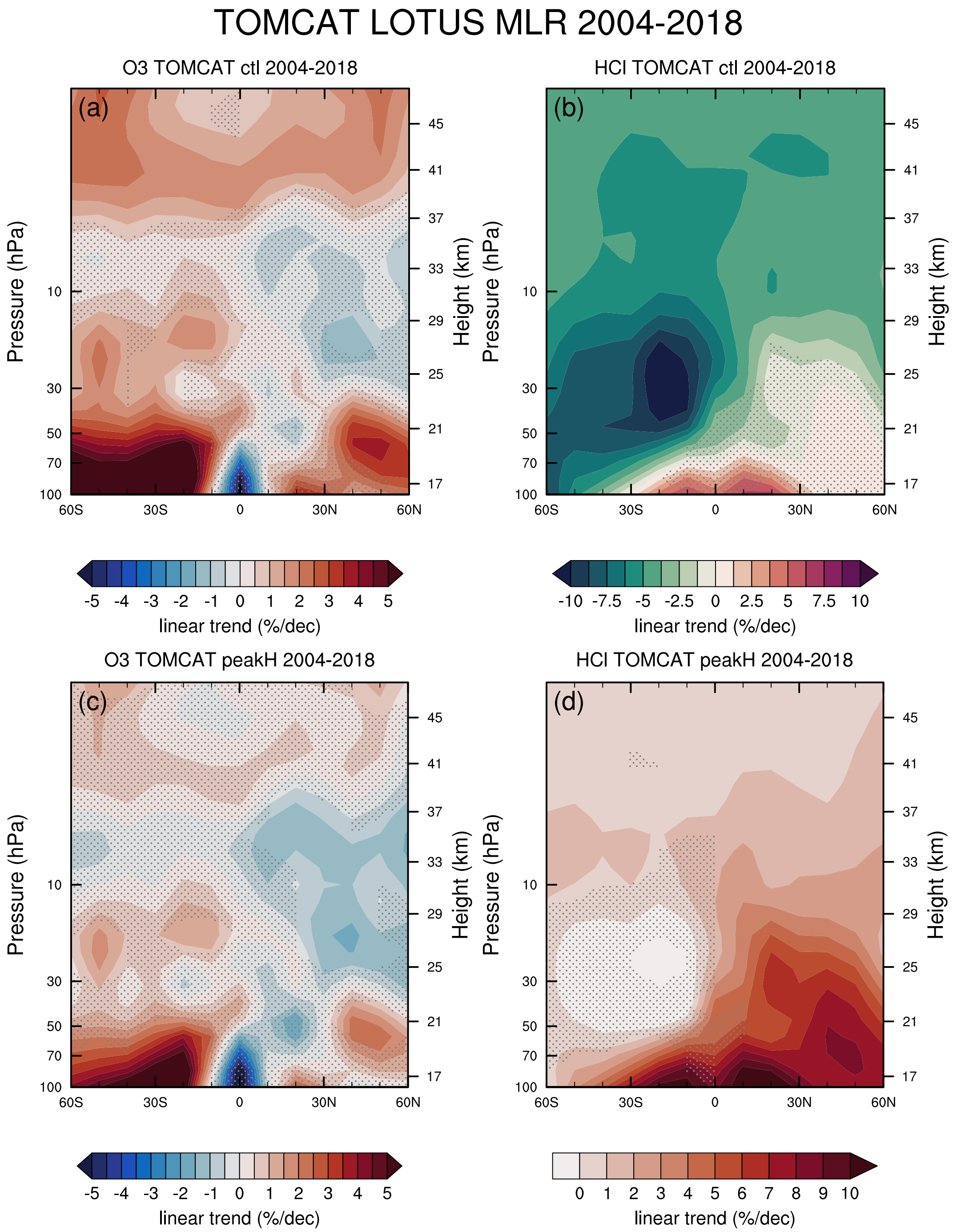

Figure 2. LOTUS multiple-linear regression trends (% dec^{-1}) between 2004 and 2018 for the TOMCAT simulations (a), (b) CTL and (c), (d) PeakH. Panels (a) and (c) show O_3; panels (b) and (d) show HCl. Gray stippling indicates where the linear trends are not statistically significant at the 95th percentile.

through 2018). Conversely, through 2021, the situation reverses, as the modeled HCl trend reaches positive values in stark contrast to the strong negative HCl trend seen in the observations. Despite an almost six-fold over-estimation of the rate by TOMCAT, both model and observations agree on an overall decreasing HCl trend over 2004–2018. Over the extended period through 2021 these discrepancies balance out across the LS, indicating a much better agreement in the decreasing HCl trends through 2021, as the reduced rate of the modeled HCl trend converges with the enhanced rate of the negative HCl trend in the observations. The latter complicated pattern of

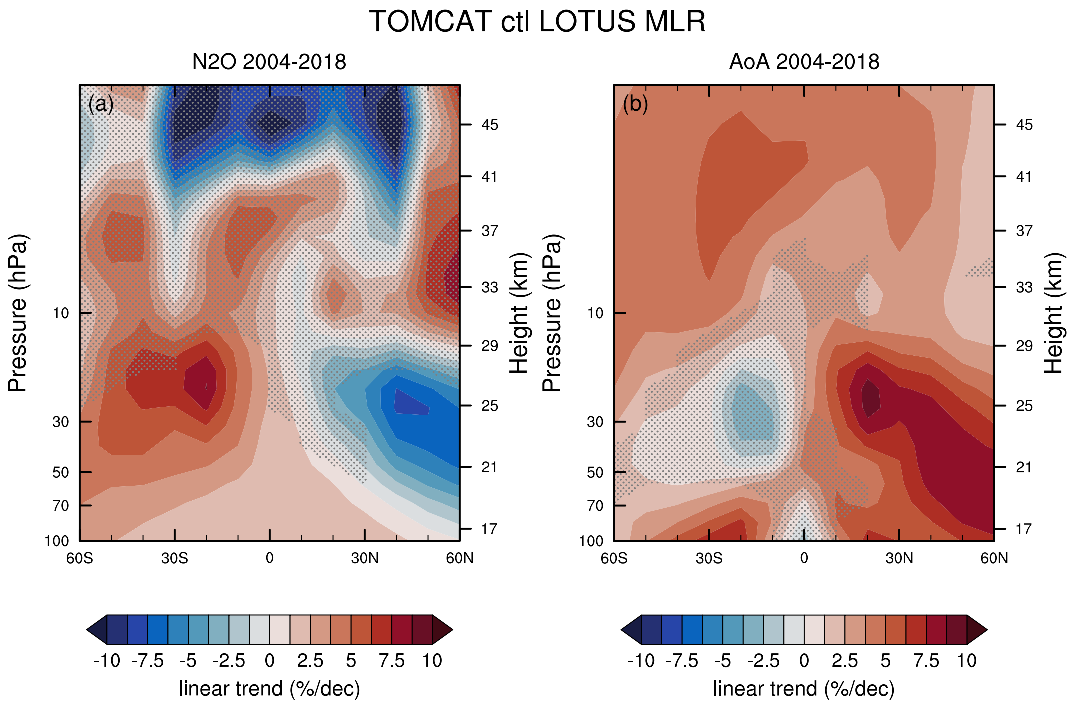

Figure 3. Trends (% dec^{-1}) for LOTUS multiple-linear regression for (a) N_2O and (b) age of air between 2004 and 2018 for the TOMCAT CTL simulation. Gray stippling indicates where the linear trends are not statistically significant at the 95th percentile.

the differing rates of the observed (modeled) HCl trends is reflected in their LS O_3 trends, showing a deceleration (acceleration) in their respective O_3 recovery rates suggesting that chemical interplay is not the dominant factor in driving the O_3 trends of the region. In LS mid-latitudes, modeled O_3 trends are 4.3% dec^{-1} in the SH and 2.2% dec^{-1} in the NH, 2–3 times larger than observations, but over 2004–2021 these discrepancies are largely improved. However, in the tropics, modeled O_3 trends (1.1% dec^{-1}) are more closely aligned to the observations (0.75% dec^{-1}) despite the increased uncertainty in the region arising from the limited coverage of ACE-FTS in the region, but through 2021, exceed 3% dec^{-1} as opposed to the very uncertain observed trends which are nearly zero, indicating significant dynamical variability influence over the extended period through 2021. This also suggests that the prescribed upper tropospheric trend in VSLS (Hossaini et al., 2019) may be too strong. In the tropical LS, the dynamical variability is a more influential factor than chlorine chemistry for O_3 changes leading to an apparent disconnect between the modeled HCl and O_3 trends in the same region.

Figure 2 and Figure S1 also show the trends in modeled O_3 and HCl from simulation PeakH. The overall negative trend in HCl (e.g., in the US) has been largely removed, but the dynamically driven interhemispheric asymmetry in the LS remains. Similarly, the overall positive (recovery) trend in O_3 has been largely removed so that in the LS, the SH shows a smaller positive trend than run CTL, while in the NH the negative trend is more negative.

Investigation of the variability and trend differences between the 2004–2018 and 2019–2021 periods (Figures S3-S16 in Supporting Information S1) clearly indicates that the notion of a single linear trend is not sufficient to describe the overall trend for 2004–2021. This justifies the focus of our study on the 2004–2018 period where the interhemispheric asymmetry signal maximizes. Internal variability can significantly influence linear trend estimates as adding or removing a few years can alter results, particularly in regions with strong dynamical variability such as the LS. Indeed, Abalos et al. (2021) highlight that internal variability, an inherent feature of atmospheric dynamics, can strongly influence tracer trends and their interpretation, showcasing its impact on modeled AoA trends. Our analysis corroborates this in the non-linear and regionally specific tracer and circulation changes when comparing the ordinary least squares O_3, HCl, N_2O and AoA (where applicable) linear trends and variability between the two periods for both ACE-FTS and TOMCAT CTL model output (Figures S3-S16 in Supporting Information S1). We find that the 2019–2021 variability remains within the broader 2004–2018 range, and that the general linear trend patterns are captured reasonably well. This trend sensitivity to the internal variability is

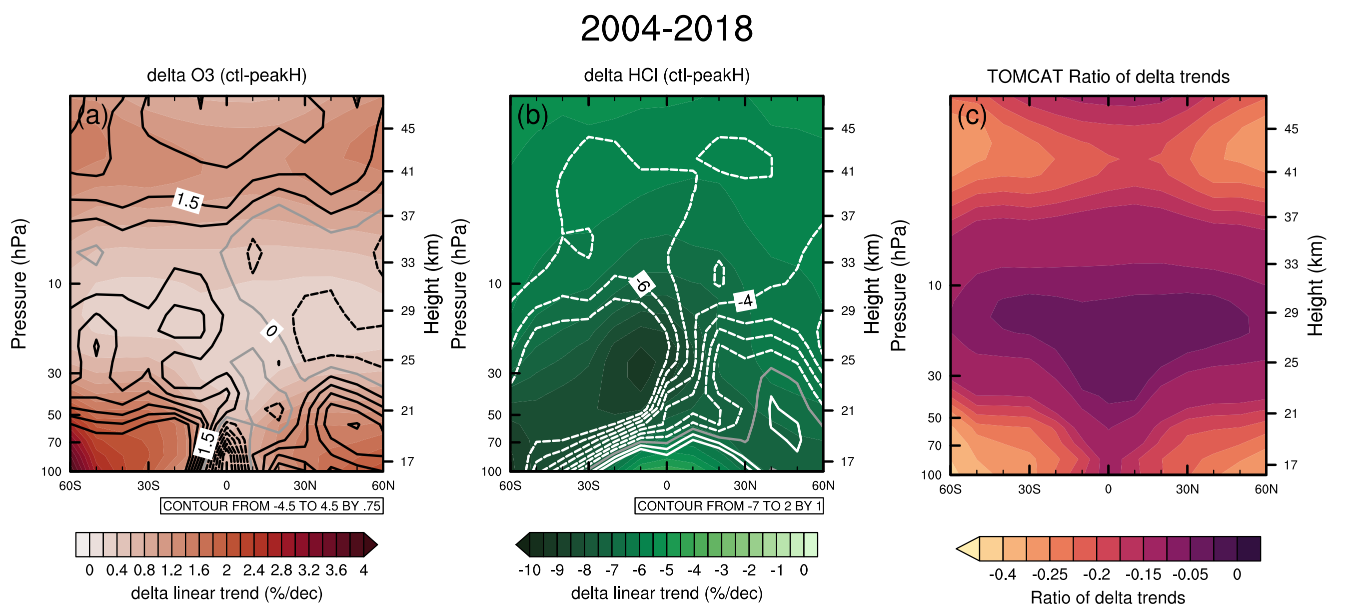

Figure 4. Differences in the 2004–2018 LOTUS multiple-linear regression linear trends (% dec^{-1}) between the TOMCAT CTL and PeakH simulations for (a) O_3 and (b) HCl. Panel (c) shows the ratio of trends shown in panels (a) and (b) (O_3 trend difference divided by HCl trend difference, termed as TOMCAT Ratio of delta trends). Overlaid solid (dashed) contours in panels (a, black) and (b, white) indicate where the TOMCAT CTL linear trends for the species plotted are positive (negative), respectively. The zero isoline is indicated by a gray solid contour in panels (a) and (b).

also well-documented, for example, by Ball et al. (2019) who demonstrated how starting and ending points can shift estimated trends even within the dynamical linear modeling (DLM) framework. Additionally, as noted by Bognar et al. (2022), trends derived from MLR analyses are comparable to those obtained via DLM, supporting the robustness of simpler linear approaches in capturing overall patterns.

Discrepancies between observations and TOMCAT results stem in part from the limitations of reanalyses driving the CTM. Reanalysis products, such as ERA5 (Hersbach et al., 2020) used here and ERA-Interim (Dee et al., 2011) used in previous studies with TOMCAT (Chipperfield et al., 2018; Mahieu et al., 2014), are not definitive representations of the BDC. They exhibit diverse transport structures, as shown in their AoA patterns and trends (Chabrillat et al., 2018; Dube et al., 2024; Ploeger et al., 2019; Ploeger & Garny, 2022) and they are also characterized by some discrepancies with balloon observations (Engel et al., 2017). Ultimately, these uncertainties project onto the CTM-modeled stratospheric composition trends. Reanalysis discrepancies can arise from differences in the representation of processes such as gravity wave drag and assimilated datasets (e.g., temperature, radiances, ozone profiles) through biases or step changes they introduce. Additionally, differences between the spatial resolution of reanalysis output, regridded to be used as input to the CTMs, can further impact simulated transport and upwelling rates (Fujiwara et al., 2022; Hassler et al., 2022).

Comparison of simulations CTL and PeakH allows us to derive a modeled sensitivity of ozone to chlorine (and concurrent changes in bromine) in different regions. To this end, differences of the modeled linear trends for 2004–2018 from the two simulations are calculated for O_3 and HCl (Figure 4). The period 2004–2021 is shown in Figure S17 in Supporting Information S1. The relatively smooth variations in the differences as a function of latitude and altitude demonstrate that the dynamical variability seen in Figure 2 (and shown in Figures 4a and 4b as contour lines) has been removed. These differences then allow us to derive the relative model sensitivity of O_3 trends to halogen (chlorine and bromine) trends (as measured by the HCl trend) in the form of the ratio of the trends (Figure 4c). The analysis reveals the expected regions of highest sensitivity as (a) the upper stratosphere where the catalytic cycle ClO + O is important for O_3 loss and (b) the mid-high latitude LS where springtime chemical loss in the polar regions (not shown) is dominated by cycles involving ClO + ClO and ClO + BrO. This polar loss can impact mid-latitudes by export of processed air (high in active chlorine and/or low in O_3). The middle stratosphere, where O_3 loss is dominated by NO_x chemistry, is a region of relatively low sensitivity to chlorine trends.

10.1029/2024JD042161

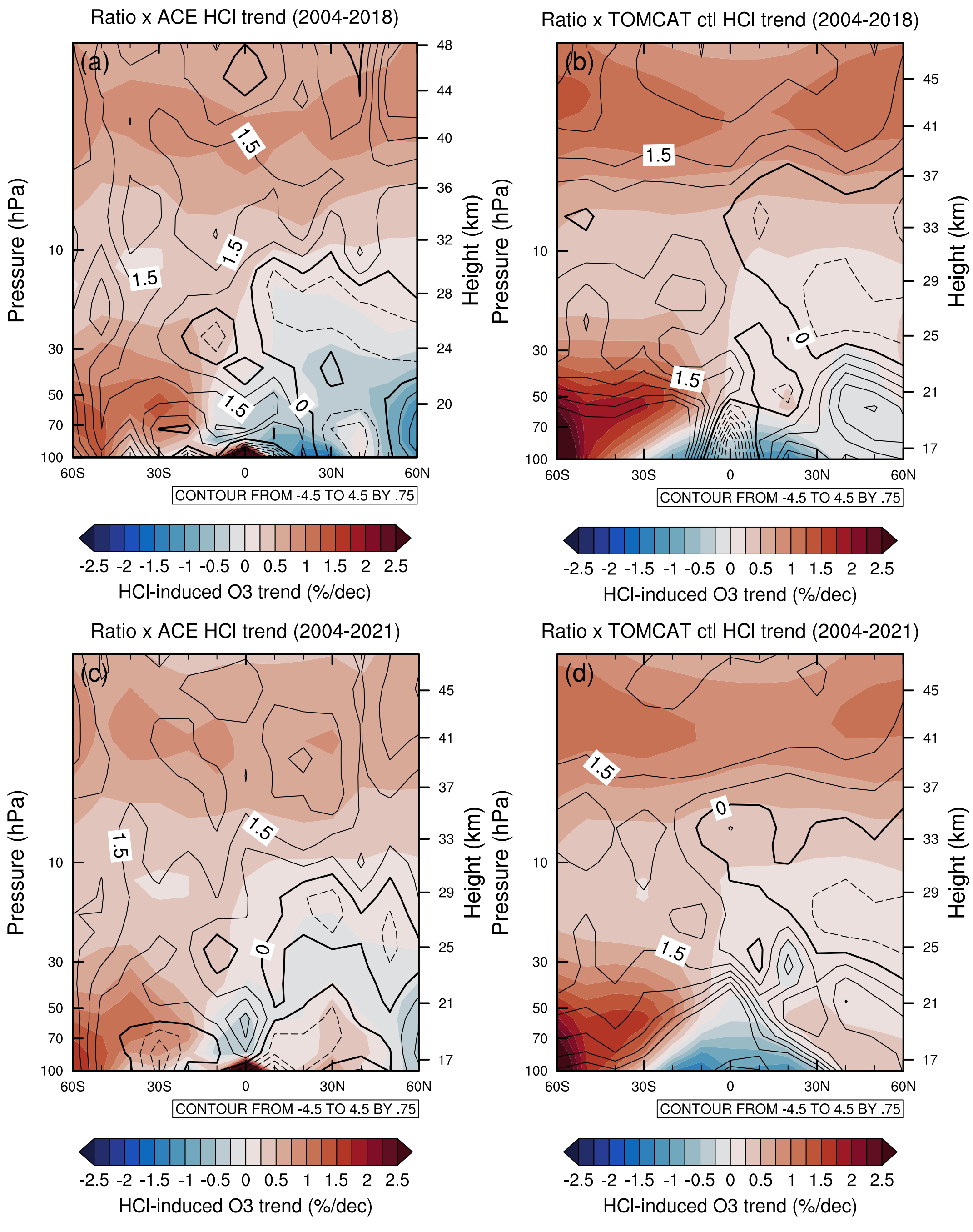

Figure 5. Panels (a) and (b) show the chlorine-induced O_3 linear trend as computed by the TOMCAT ratio (Figure 4c) multiplied with the atmospheric chemistry experiment - fourier transform spectrometer (ACE-FTS) and TOMCAT CTL HCl trends, respectively, for the period 2004–2018. Panels (c) and (d) are the equivalent plots for 2004–2021 where the TOMCAT ratio is taken from Figure S17c in Supporting Information S1. Black solid (dashed) contours indicate the regions where the ACE-FTS or TOMCAT CTL O_3 linear trend is positive (negative), respectively, with zero shown as the thickest contour.

The model-derived sensitivity of O_3 to chlorine and bromine under recent conditions (Figure 4) allows us to estimate the contribution of halogen chemistry (using HCl as the proxy) to the recent O_3 trends. For both ACE-FTS and TOMCAT, the HCl trend is multiplied with the modeled O_3/HCl sensitivity to derive the fraction of the O_3 trend due to halogen chemistry as seen in Figure 5 (for both 2004–2018 and 2004–2021; the equivalent percentage plots are presented in Figure S18 in Supporting Information S1) and the estimates for different

Table 1
Latitudinally Averaged HCl-Induced O_3 Trends (% Dec^{-1}) for Both LS/US Atmospheric Chemistry Experiment - Fourier Transform Spectrometer (ACE-FTS) and TOMCAT CTL for 2004–2018 and 2004–2021

	2004–2018		2004–2021	
Stratospheric layer and region	ACE-FTS	TOMCAT CTL	ACE-FTS	TOMCAT CTL
LS SH mid-lats	0.98	1.82	1.02	1.60
LS NH mid-lats	−0.55	−0.06	−0.14	0.21
LS Tropics	0.21	0.04	0.26	−0.15
LS Average	0.21	0.50	0.38	0.45
US SH mid-lats	0.64	0.88	0.62	0.83
US NH mid-lats	0.63	0.82	0.53	0.75
US Tropics	0.62	0.72	0.56	0.66
US Average	0.62	0.79	0.57	0.73

latitudinal regions in the LS (100–31.62 hPa) and US over both 2004–2018 and 2004–2021 are presented bellow in Table 1.

In the US, the derived trends in Table 1 are positive and account for the majority of the observed O_3 trend, confirming the dominant influence of halogens (specifically chlorine) to ozone recovery in this region. Over 2004–2018, the model based estimate of the HCl-induced O_3 trend explains on average 0.62% dec^{-1} out of the ACE-FTS US O_3 trend of 1.36% dec^{-1} (Figure 5a). In contrast, over the full 2004–2021 period, the equivalent amount explained by the model O_3/HCl sensitivity is decreased as the observed O_3 trend in the region shows an increased rate of recovery that cannot be explained by chlorine chemistry alone. A similar picture is seen, albeit to a lesser degree, in the TOMCAT O_3 trends and their contributions from the model-derived HCl-induced O_3 trend in the extrapolar US. Naturally, the latter explain almost all the TOMCAT US O_3 trend over 2004–2018 (Figure 5b) however, this estimate decreases through 2021 where the derived HCl-induced O_3 trend contributes an 0.8% dec^{-1} of the simulated 1.1% dec^{-1} of the US region. Therefore, we can attribute at least two-thirds of the modeled US O_3 recovery to the chlorine decrease, almost double that for the ACE-FTS (over 2004–2021), although note that our offline CTM necessarily ignores feedback of the Cl-induced ozone change. The other important contribution in the O_3 increase of the US region is from cooling (Maycock et al., 2018; Randel et al., 2016). The values of the model O_3/HCl sensitivity contribution to the observed and modeled O_3 trends maximize in the SH mid-lats and exhibit a small variance of up to 0.2% dec^{-1} within the broad regions of US layer for both ACE-FTS and TOMCAT, a feature associated with the uniform decrease in the modeled HCl trends (Figure 2b) in the region. Overall, in the US, for both ACE-FTS and TOMCAT, these derived trends are slightly reduced when compared to their equivalent contributions to the O_3 trends over 2004–2021 suggesting a suppressed chemical contribution in their respective O_3 recovery rates.

In the LS, the derived ozone trends clearly follow the interhemispheric asymmetry in the observed and modeled HCl trends, scaled by the sensitivity of O_3 to HCl, which accentuates the changes in the polar regions (not shown). Over 2004–2018, for ACE-FTS, the modeled chemical impact of the dynamically induced asymmetry is to enhance the strong positive mid-latitude O_3 recovery signal in the SH (by ∼1% dec^{-1}) and to decrease the negligible signal in the NH by about −0.55% dec^{-1}. For TOMCAT, the derived chemical contribution to the O_3 trend maximizes in the SH cell reaching 1.8% dec^{-1} compared to the very strong modeled trend in the region (4.3% dec^{-1}). Conversely, in the tropics and the NH cell, the chemically induced trend is essentially zero, which for the latter is associated with the enhanced dynamical variability of the region compared to the SH. However, over the extended period 2004–2021, in ACE-FTS, the suppression of the interhemispheric asymmetry reinforces the chlorine influence projecting onto the O_3 trends, a feature reflected mostly in the SH cell, while for TOMCAT the overall contribution of the HCl-induced O_3 trends shows an overall reduction compared to 2004–2018. The above can be attributed mainly to the non-linear and asymmetric changes in both the observed and modeled trends arising mostly from the tropical and NH mid-lat regions when including the remaining years through 2021. Moreover, the interhemispheric asymmetry of the lower to middle stratosphere is larger for the 2004–2018 period compared to 2004–2021 as seen from the observed N_2O trends (Figure 1). Accordingly, the chemical impact of the asymmetric HCl changes is stronger for 2004–2018 (Figure 5) leading to halogen-driven negative O_3 trends in the NH midlatitudes for both, ACE-FTS (-0.6% dec^{-1}) and TOMCAT to a lesser degree.

4. Conclusions

Our analysis of ACE-FTS satellite observations, complemented by TOMCAT model simulations, underscores the differentiated behavior of O_3, HCl and N_2O across different layers in the stratosphere and the critical role of dynamical variability in driving the trends of these gases. This ultimately reveals important insights into the complex interplay between chemistry and dynamics in the stratosphere.

In the mid-upper stratosphere (above 10 hPa), ACE-FTS data show a clear negative HCl trend averaging -4% dec^{-1} over 2004–2018, slightly more negative than the 2004–2021 period, reflecting the reduction in stratospheric chlorine due to the Montreal Protocol. This decrease contributes to an O_3 increase of 1.36% dec^{-1} over 2004–2018, which is less positive than the longer period through 2021. The well-mixed greenhouse gas N_2O also shows a significant increase in the mid-upper stratosphere, driven by continuing tropospheric increases. In the LS, O_3, HCl, and N_2O trends display interhemispheric asymmetries. Positive (negative) N_2O trends in SH (NH) reflect the stratospheric transport variability. HCl trends show a strong negative trend in the SH and a moderate positive trend in the NH, while O_3 trends increase strongly in the SH but show no significant change in the NH, which has become more positive over the extended period. These trends result from both dynamical variability and changes in halogen composition. Model simulations for 2004–2018 largely agree with these observations, showing a relatively uniform decrease in HCl in the upper stratosphere. However, the model's O_3 trend in this region is about two-thirds of the observed trend, and its HCl trends are more negative. In the LS, despite some discrepancies in the NH, the model captures the observed hemispheric asymmetry but with weaker amplitude. The AoA trends suggest a slowdown in stratospheric circulation from 2019 to 2021.

In the LS, modeled HCl trends are -7.4% dec^{-1} in the SH mid-latitudes, significantly lower than observations. NH mid-latitudes show differences of equal magnitude, but model and observations agree on the sign of their trends. In the tropics, model and observations show trends of opposite sign alternating between over two periods considered here; ACE-FTS exhibits a small positive trend, and the model shows a moderate decreasing trend through 2018, with a reversal manifesting through 2021. These discrepancies do not necessarily balance out over the period that the interhemispheric asymmetry maximizes, but indicate an overall decreasing HCl trend through 2018 despite their different rates, with an increased (decreased) rate for observations (model) compared to 2004–2021 where there is a much better agreement. This reduction is reflected in the O_3 trends, showing a slowdown in the simulated rate of O_3 recovery. Modeled O_3 trends in the LS mid-latitudes are larger than observed and show increased biases with observations compared to 2004–2018.

It is crucial to underscore that this study is principally conceptual in nature, with the objective of elucidating the influence of transport-induced alterations in chlorine loading on ozone trends. Although we present linear trend estimates, our primary objective is to understand the mechanisms responsible for the observed changes in ozone levels, rather than to achieve highly precise or robust trend quantification. This conceptual approach enables the observed trends to be contextualized within the broader framework of dynamical and chemical processes. The derived numbers are contingent upon the model employed, as discrepancies in transport representation and tracer trends may originate from biases in the meteorological input data, such as reanalysis products like ERA5. Moreover, the selected period exerts a pronounced influence on the outcomes, with internal variability, particularly in the LS, modulating trends based on the choice of start and end dates. These factors underscore the necessity of interpreting the trends within the context of model-specific limitations and inherent variability in the input data.

The TOMCAT model simulations help elucidate the impact of dynamical variability on these trends and indicate that chlorine chemistry significantly influences O_3 recovery in the upper stratosphere. In the LS, the derived O_3 trends follow the interhemispheric asymmetry in HCl trends, enhancing the SH mid-latitude O_3 recovery and offsetting it in the NH. This highlights the combined impact of chemical and dynamical processes on recent O_3 trends. These trends are influenced by multiannual variability in transport processes, as evidenced by the similar patterns between observations and model output in their respective N_2O and HCl trends.

Data Availability Statement

TOMCAT model data is available at https://doi.org/10.5281/zenodo.12595192 (Chrysanthou, 2024 Zenodo, uploaded 2024-06-30). Atmospheric chemistry experiment - fourier transform spectrometer v4.1/v4.2 data are available at https://databace.scisat.ca/level2/. Atmospheric chemistry experiment - fourier transform spectrometer v4.1/v4.2 data quality flags are available at https://doi.org/10.5683/SP2/BC4ATC (P. Sheese & Walker, 2020).

The LOTUS regression code and documentation is available at https://arg.usask.ca/docs/LOTUS_regression/index.html (last access: 27/06/2024).

Acknowledgments

AC and MPC were supported by the Natural Environment Research Council (NERC) LSO3 (NE/V011863/1) and ESA OREGANO (4000137112/22/I-AG) projects. The work in Leeds was also supported by NERC NCEO. We thank Wuhu Feng (NCAS Leeds) for help with the model and Sandip Dhomse (NCEO Leeds) for discussions. The simulations were performed on the Leeds ARC and UK Archer2 HPC systems. KD is supported by the Canadian Space Agency (Grant 21SUASULSO). The Atmospheric Chemistry Experiment (ACE) is a Canadian-led mission mainly supported by the CSA and the NSERC, and Peter Bernath is the principal investigator.

References

Abalos, M., Calvo, N., Benito-Barca, S., Garny, H., Hardiman, S. C., Lin, P., et al. (2021). The brewer–dobson circulation in CMIP6. *Atmospheric Chemistry and Physics*, *21*(17), 13571–13591. https://doi.org/10.5194/acp-21-13571-2021

Abalos, M., Polvani, L., Calvo, N., Kinnison, D., Ploeger, F., Randel, W., & Solomon, S. (2019). New insights on the impact of ozone-depleting substances on the brewer-dobson circulation. *Journal of Geophysical Research: Atmospheres*, *124*(5), 2435–2451. https://doi.org/10.1029/2018JD029301

Ball, W. T., Alsing, J., Mortlock, D. J., Staehelin, J., Haigh, J. D., Peter, T., et al. (2018). Evidence for a continuous decline in lower stratospheric ozone offsetting ozone layer recovery. *Atmospheric Chemistry and Physics*, *18*(2), 1379–1394. https://doi.org/10.5194/acp-18-1379-2018

Ball, W. T., Alsing, J., Staehelin, J., Davis, S. M., Froidevaux, L., & Peter, T. (2019). Stratospheric ozone trends for 1985-2018: Sensitivity to recent large variability. *Atmospheric Chemistry and Physics*, *19*(19), 12731–12748. https://doi.org/10.5194/acp-19-12731-2019

Bernath, P. F., McElroy, C. T., Abrams, M. C., Boone, C. D., Butler, M., Camy-Peyret, C., et al. (2005). Atmospheric chemistry experiment (ACE): Mission overview. *Geophysical Research Letters*, *32*(15), 1–5. https://doi.org/10.1029/2005GL022386

Bognar, K., Tegtmeier, S., Bourassa, A., Roth, C., Warnock, T., Zawada, D., & Degenstein, D. (2022). Stratospheric ozone trends for 1984-2021 in the SAGE II-OSIRIS-SAGE III/ISS compositedataset. *Atmospheric Chemistry and Physics*, *22*(14), 9553–9569. https://doi.org/10.5194/acp-22-9553-2022

Boone, C. D., Bernath, P. F., Cok, D., Jones, S. C., & Steffen, J. (2020). Version 4 retrievals for the atmospheric chemistry experiment Fourier transform spectrometer (ACE-FTS) and imagers. *Journal of Quantitative Spectroscopy and Radiative Transfer*, *247*, 106939. https://doi.org/10.1016/j.jqsrt.2020.106939

Boone, C. D., Nassar, R., Walker, K. A., Rochon, Y., McLeod, S. D., Rinsland, C. P., & Bernath, P. F. (2005). Retrievals for the atmospheric chemistry experiment Fourier-transform spectrometer. *Applied Optics*, *44*(33), 7218–7231. https://doi.org/10.1364/AO.44.007218

Chabrillat, S., Vigouroux, C., Christophe, Y., Engel, A., Errera, Q., Minganti, D., et al. (2018). Comparison of mean age of air in five reanalyses using the BASCOE transport model. *Atmospheric Chemistry and Physics*, *18*(19), 14715–14735. https://doi.org/10.5194/acp-18-14715-2018

Chipperfield, M. P. (2006). New version of the TOMCAT/SLIMCAT off-line chemical transport model: Intercomparison of stratospheric tracer experiments. *Quarterly Journal of the Royal Meteorological Society*, *132*(617), 1179–1203. https://doi.org/10.1256/qj.05.51

Chipperfield, M. P., Bekki, S., Dhomse, S., Harris, N. R. P., Hassler, B., Hossaini, R., et al. (2017). Detecting recovery of the stratospheric ozone layer. *Nature*, *549*(7671), 211–218. https://doi.org/10.1038/nature23681

Chipperfield, M. P., Dhomse, S., Hossaini, R., Feng, W., Santee, M. L., Weber, M., et al. (2018). On the cause of recent variations in lower stratospheric ozone. *Geophysical Research Letters*, *45*(11), 5718–5726. https://doi.org/10.1029/2018GL078071

Chrysanthou, A. (2024). Hemispheric asymmetry in stratospheric trends of HCl and ozone: Impact of chemical feedback on ozone recovery [Dataset]. *Zenodo*. https://doi.org/10.5281/ZENODO.12595193

Dee, D. P., Uppala, S. M., Simmons, A. J., Berrisford, P., Poli, P., Kobayashi, S., et al. (2011). The ERA-interim reanalysis: Configuration and performance of the data assimilation system. *Quarterly Journal of the Royal Meteorological Society*, *137*(656), 553–597. https://doi.org/10.1002/qj.828

Dhomse, S. S., Feng, W., Montzka, S. A., Hossaini, R., Keeble, J., Pyle, J. A., et al. (2019). Delay in recovery of the Antarctic ozone hole from unexpected CFC-11 emissions. *Nature Communications*, *10*(1), 1–12. https://doi.org/10.1038/s41467-019-13717-x

Dubé, K., Randel, W., Bourassa, A., Zawada, D., McLinden, C., & Degenstein, D. (2020). Trends and variability in stratospheric NOx derived from merged SAGE II and OSIRIS satellite observations. *Journal of Geophysical Research: Atmospheres*, *125*(7), e2019JD031798. https://doi.org/10.1029/2019jd031798

Dubé, K., Tegtmeier, S., Bourassa, A., Zawada, D., Degenstein, D., Sheese, P. E., et al. (2023). N2O as a regression proxy for dynamical variability in stratospheric trace gas trends. *Atmospheric Chemistry and Physics*, *23*(20), 13283–13300. https://doi.org/10.5194/acp-23-13283-2023

Dube, K., Tegtmeier, S., Ploeger, F., & Walker, K. A. (2024). Hemispheric asymmetry in recent stratospheric age of air changes. *EGUsphere*, *3*(Issue x), 1–21. https://doi.org/10.5194/egusphere-2024-1736

Engel, A., Bönisch, H., Ullrich, M., Sitals, R., Membrive, O., Danis, F., & Crevoisier, C. (2017). Mean age of stratospheric air derived from AirCore observations. *Atmospheric Chemistry and Physics*, *17*(11), 6825–6838. https://doi.org/10.5194/acp-17-6825-2017

Fujiwara, M., Manney, G. L., Gray, L. J., & Wright, C. J. (Eds.) (2022). SPARC, 2022: SPARC reanalysis intercomparison project (S-rip) final report, *SPARC report No. 10, WCRP-17/2020*. available at. https://doi.org/10.17874/800dee57d13

Galytska, E., Rozanov, A., Chipperfield, M. P., Dhomse, S. S., Weber, M., Arosio, C., et al. (2019). Dynamically controlled ozone decline in the tropical mid-stratosphere observed by SCIAMACHY. *Atmospheric Chemistry and Physics*, *19*(2), 767–783. https://doi.org/10.5194/acp-19-767-2019

Han, Y., Tian, W., Chipperfield, M. P., Zhang, J., Wang, F., Sang, W., et al. (2019). Attribution of the hemispheric asymmetries in trends of stratospheric trace gases inferred from microwave limb sounder (MLS) measurements. *Journal of Geophysical Research: Atmospheres*, *124*(2006), 6283–6293. https://doi.org/10.1029/2018JD029723

Harris, N. R. P., Hassler, B., Tummon, F., Bodeker, G. E., Hubert, D., Petropavlovskikh, I., et al. (2015). Past changes in the vertical distribution of ozone - Part 3: Analysis and interpretation of trends. *Atmospheric Chemistry and Physics*, *15*(17), 9965–9982. https://doi.org/10.5194/acp-15-9965-2015

Hassler, B., Young, P. J., Ball, W. T., Damadeo, R., Keeble, J., Maillard Barras, E., et al. (2022). Update on global ozone: Past, present, and future, chapter 3. GAW Report No. In *Scientific assessment of ozone depletion: 2022* (Vol. 278, p. 56). WMO.
Hersbach, H., Bell, B., Berrisford, P., Hirahara, S., Horányi, A., Muñoz-Sabater, J., et al. (2020). The ERA5 global reanalysis. *Quarterly Journal of the Royal Meteorological Society*, *146*(730), 1999–2049. https://doi.org/10.1002/qj.3803
Hossaini, R., Atlas, E., Dhomse, S. S., Chipperfield, M. P., Bernath, P. F., Fernando, A. M., et al. (2019). Recent trends in stratospheric chlorine from very short-lived substances. *Journal of Geophysical Research: Atmospheres*, *124*(4), 2318–2335. https://doi.org/10.1029/2018JD029400
Kovilakam, M., Thomason, L. W., Ernest, N., Rieger, L., Bourassa, A., & Millán, L. (2020). The global space-based stratospheric aerosol climatology (version 2.0): 1979–2018. *Earth System Science Data*, *12*(4), 2607–2634. https://doi.org/10.5194/essd-12-2607-2020
Kyrölä, E., Laine, M., Sofieva, V., Tamminen, J., Pivrinta, S. M., Tukiainen, S., et al. (2013). Combined SAGE II-GOMOS ozone profile data set for 1984-2011 and trend analysis of the vertical distribution of ozone. *Atmospheric Chemistry and Physics*, *13*(21), 10645–10658. https://doi.org/10.5194/acp-13-10645-2013
Mahieu, E., Chipperfield, M. P., Notholt, J., Reddmann, T., Anderson, J., Bernath, P. F., et al. (2014). Recent Northern Hemisphere stratospheric HCl increase due to atmospheric circulation changes. *Nature*, *515*(7525), 104–107. https://doi.org/10.1038/nature13857
Maycock, A. C., Randel, W. J., Steiner, A. K., Karpechko, A. Y., Christy, J., Saunders, R., et al. (2018). Revisiting the mystery of recent stratospheric temperature trends. *Geophysical Research Letters*, *45*(18), 9919–9933. https://doi.org/10.1029/2018GL078035
Newchurch, M. J., Yang, E. S., Cunnold, D. M., Reinsel, G. C., Zawodny, J. M., & Russell, J. M. (2003). Evidence for slowdown in stratospheric ozone loss: First stage of ozone recovery. *Journal of Geophysical Research*, *108*(16), 1–13. https://doi.org/10.1029/2003jd003471
Ploeger, F., & Garny, H. (2022). Hemispheric asymmetries in recent changes in the stratospheric circulation. *Atmospheric Chemistry and Physics*, *22*(8), 5559–5576. https://doi.org/10.5194/acp-22-5559-2022
Ploeger, F., Legras, B., Charlesworth, E., Yan, X., Diallo, M., Konopka, P., et al. (2019). How robust are stratospheric age of air trends from different reanalyses? *Atmospheric Chemistry and Physics*, *19*(9), 6085–6105. https://doi.org/10.5194/acp-19-6085-2019
Polvani, L. M., Abalos, M., Garcia, R., Kinnison, D., & Randel, W. J. (2018). Significant weakening of brewer-dobson circulation trends over the 21st century as a consequence of the Montreal Protocol. *Geophysical Research Letters*, *45*(1), 401–409. https://doi.org/10.1002/2017GL075345
Prather, M. J., Froidevaux, L., & Livesey, N. J. (2023). Observed changes in stratospheric circulation: Decreasing lifetime of N2O, 2005-2021. *Atmospheric Chemistry and Physics*, *23*(2), 843–849. https://doi.org/10.5194/acp-23-843-2023
Prignon, M., Chabrillat, S., Friedrich, M., Smale, D., Strahan, S. E., Bernath, P. F., et al. (2021). Stratospheric fluorine as a tracer of circulation changes: Comparison between infrared remote-sensing observations and simulations with five modern reanalyses. *Journal of Geophysical Research: Atmospheres*, *126*(19), 1–24. https://doi.org/10.1029/2021jd034995
Randel, W. J., Smith, A. K., Wu, F., Zou, C. Z., & Qian, H. (2016). Stratospheric temperature trends over 1979-2015 derived from combined SSU, MLS, and SABER satellite observations. *Journal of Climate*, *29*(13), 4843–4859. https://doi.org/10.1175/JCLI-D-15-0629.1
Sheese, P., & Walker, K. (2020). Data quality flags for ACE-FTS level 2 version 4.1/4.2 data set. *Scholars Portal Dataverse*, *V2*. [DataSet]. https://doi.org/10.5683/SP2/BC4ATC
Sheese, P. E., Boone, C. D., & Walker, K. A. (2015). Detecting physically unrealistic outliers in ACE-FTS atmospheric measurements. *Atmospheric Measurement Techniques*, *8*(2), 741–750. https://doi.org/10.5194/amt-8-741-2015
Sofieva, V. F., Kyrölä, E., Laine, M., Tamminen, J., Degenstein, D., Bourassa, A., et al. (2017). Merged SAGE II, Ozone_cci and OMPS ozone profile dataset and evaluation of ozone trends in the stratosphere. *Atmospheric Chemistry and Physics*, *17*(20), 12533–12552. https://doi.org/10.5194/acp-17-12533-2017
Solomon, S., Ivy, D. J., Kinnison, D., Mills, M. J., Neely, R. R., & Schmidt, A. (2016). Emergence of healing in the Antarctic ozone layer. *Science*, *353*(6296), 269–274. https://doi.org/10.1126/science.aae0061
Steinbrecht, W., Froidevaux, L., Fuller, R., Wang, R., Anderson, J., Roth, C., et al. (2017). An update on ozone profile trends for the period 2000 to 2016. *Atmospheric Chemistry and Physics*, *17*(17), 10675–10690. https://doi.org/10.5194/acp-17-10675-2017
Steiner, A. K., Ladstädter, F., Randel, W. J., Maycock, A. C., Fu, Q., Claud, C., et al. (2020). Observed temperature changes in the troposphere and stratosphere from 1979 to 2018. *Journal of Climate*, *33*(19), 1–72. https://doi.org/10.1175/JCLI-D-19-0998.1
Stiller, G. P., Fierli, F., Ploeger, F., Cagnazzo, C., Funke, B., Haenel, F. J., et al. (2017). Shift of subtropical transport barriers explains observed hemispheric asymmetry of decadal trends of age of air. *Atmospheric Chemistry and Physics*, *17*(18), 11172–11192. https://doi.org/10.5194/acp-17-11177-2017
Stolarski, R. S., Douglass, A. R., Remsberg, E. E., Livesey, N. J., & Gille, J. C. (2012). Ozone temperature correlations in the upper stratosphere as a measure of chlorine content. *Journal of Geophysical Research*, *117*(10), 1–8. https://doi.org/10.1029/2012JD017456
Strahan, S. E., Smale, D., Douglass, A. R., Blumenstock, T., Hannigan, J. W., Hase, F., et al. (2020). Observed hemispheric asymmetry in stratospheric transport trends from 1994 to 2018. *Geophysical Research Letters*, *47*(17), 1–9. https://doi.org/10.1029/2020gl088567
Tian, H., Pan, N., Thompson, R. L., Canadell, J. G., Suntharalingam, P., Regnier, P., et al. (2024). Global nitrous oxide budget (1980–2020). *Earth System Science Data*, *16*(6), 2543–2604. https://doi.org/10.5194/essd-16-2543-2024
WMO. (2018). (World Meteorological Organization), Scientific Assessment of Ozone Depletion: 2018. *Global Ozone Research and Monitoring Project – Report No.*, *58*.